Predicting the Formation, Structure and Elastomeric Properties of End-Linked Polymer Networks

R.F.T. Stepto*, J.I. Cail and D.J.R. Taylor

Polymer Science and Technology Group, Manchester Materials Science Centre, UMIST and University of Manchester, Grosvenor St., Manchester, M1 7HS, UK

SUMMARY: The molecular structures and macroscopic properties of network polymers depend more closely on reactant structures (molar masses, functionalities, chain flexibilities) and reaction conditions (dilution, proportions of different reactants) than do those of linear polymers. To understand and predict elastomeric properties, it is important to be able to model, statistically, the molecular growth leading to network formation. A new Monte-Carlo network polymerisation algorithm has been developed, using Flory-Stockmayer random-reaction statistics with intramolecular reaction allowed on a correctly weighted basis. The algorithm simulates, as a function of extent of reaction, the formation of *all of the connections* in a reaction mixture and counts *all* the ring structures. It also enables polymerisations and network structures to be simulated efficiently up to *complete* reaction. Comparisons of predictions from the algorithm with experimental data from end-linking polymerisations show the importance of accounting for the *whole* distribution of sizes of ring structure in determining reductions in elastic modulus. An important new factor, x, is introduced in the interpretation of experimental data. It is the fractional loss in elasticity per chain in loop structures larger than the smallest.

Perfect Network Formation

The classical Flory-Stockmayer (F-S) treatment of the gel point and the accompanying changes in distributions of molecular species give a basic explanation of the phenomena to which the behaviour and changes in actual polymerisations may be related. However, as discussed in detail by Flory[1], the infinite species which occur from the gel point to complete reaction cannot be enumerated as individual molecules. In addition, F-S theory says nothing concerning the detailed topology of the network, which grows and defines its structure through the random reaction of its reactive groups with other groups on the gel and with groups on sol species. To obtain a perfect network, all reactions (sol-sol, sol-gel and gel-gel) are assumed to yield elastically active chains between junction points in the final network. This assumption is rarely true and will be examined in detail in this paper.

The elastomeric properties of polymer networks depend to a large extent on the value of the molar mass of the elastically active chain connecting a pair of junction points, M_c. If a perfect network structure is assumed then M_c can be calculated directly from the reactant structures, taking account of unreacted groups for non-stoichiometric reaction mixtures. In general, the

 CCC 1022-1360/00/$ 17.50+.50/0

detailed relationship between M_c and reactant structures depends on reactant architectures as well as extents of reaction and it is not possible to give a completely general formula. For example, comb-like reactants with pendant reactive groups give loose ends, which are connected to only single branch points, and two types of chains between junction points, those involving sections of the backbone chains and those involving side chains. However, formulae for M_c from most stoichiometric endlinking polymerisations (using star reactants) at complete reaction can be derived relatively simply by assuming the perfect network structure and relating it to the structures of the reactants from which it is formed[2,3]. In such networks there are no loose ends and M_c is related to the molar concentration and number of moles of chains connecting pairs of junction points, n_c and N_c, respectively, by the relationships

$$n_c = \frac{N_c}{V_{net}} = \frac{N_c}{W_{net}} \cdot \frac{W_{net}}{V_{net}} = \frac{1}{M_c} \cdot \rho , \qquad (1)$$

where W_{net} and V_{net} are the mass and the volume of network, respectively, and ρ is the density of the network. It is assumed that any sol fraction has been removed. $1/M_c$ for networks formed from several reactants is an average value, denoted $<1/M_c>$, and may be related to reactant structures after introduction of N_J, the number of junction points in the network, to give

$$< \frac{1}{M_c} >= \frac{N_c}{N_J} \cdot \frac{N_J}{W_{net}} \quad . \qquad (2)$$

General expressions for $<1/M_c>$ may be derived[2,3] for quite complex polymerisations, e.g. $\Sigma_i RA_{fai} + \Sigma_j R'B_{fbj}$ polymerisations. However, for present purposes, considerations are limited to $RA_2 + R'B_f$ polymerisations. In that case,

$$\frac{N_c}{N_J} = \frac{f}{2} \quad , \qquad (3)$$

as $f/2$ chains emanate from each junction and M_c (= W_{net}/N_c) is simply the molar mass of two arms of the $R'B_f$ unit plus the molar mass of the RA_2 unit.

Relationships between concentrations of chains and junction points that assume perfect network structures, such as equations (1) to (3), are often used when interpreting elastic properties of endlinked networks[4]. All chains and junction points are assumed to be elastically active. In this case, one may replace the symbols N_c and N_J by N_{ec} and N_{eJ}, denoting the numbers of elastically active chains and junction points. In practice, deviations from these assumptions occur and the values of N_{ec} or N_{eJ} deduced from elastomeric properties are rarely those expected from the amount of chemical reaction that has occurred. Such deviations may be due to topological entanglements and chain interactions[5-9], to side

reactions, incomplete reaction in endlinking polymerisations (giving loose ends)[10,11] and, more fundamentally and generally, inelastic chain or loop formation due to the intramolecular reaction of pairs of groups[2,3,9].

It is obviously important for predicting and interpreting the elastomeric properties of networks to be able to calculate the value of N_{ec} , N_{eJ} or M_c from the reactants and the reaction conditions used. For stoichiometric RA_2 + $R'B_f$ polymerisations at complete reaction, one may write M_c as

$$M_c^o = \frac{W_{net}}{N_{ec}^o} \quad , \tag{4}$$

where M_c^o and N_{ec}^o refer to the perfect network structure. In reality, due to intramolecular reaction the actual number of elastic chains, N_{ec} , is less than N_{ec}^o , giving

$$M_c = \frac{W_{net}}{N_{ec}} \quad , \tag{5}$$

with $M_c > M_c^o$. Thus, M_c may be considered as the key quantity to consider, both experimentally and theoretically.

Elastic Modulus

The close connection between network structures and modulus (G) is summarised by the equations, based on the application of Gaussian elasticity theory to uniaxial deformation[2-4],

$$\sigma = G(\Lambda - \Lambda^{-2}) \tag{6}$$

and

$$G = ART\rho\varphi_2^{1/3}(V_u / V_F)^{2/3} / M_c \quad . \tag{7}$$

Equations (6) and (7) are valid at relatively low deformations. G is the shear modulus measured at zero frequency. σ is the applied stress per undeformed area and Λ the experimental deformation ratio. In the absence of free chain-ends, A has the values of $(1 - 2/f)$ and 1 for phantom and affine chain behaviours, respectively. Also, A may be put equal to 1 for values of Λ near 1. ρ is the density of the dry network, ϕ_2 the volume fraction of network during measurement (ϕ_2=1 for unswollen networks having no sol fraction), V_u is the volume of the dry, unstrained network and V_F the volume at formation (assumed to be equivalent to V_o, the volume in the strain-free reference state.) Hence, values of M_c may be deduced from measurements of modulus using equation (7). For dry networks, prepared in bulk $V_u = V_F$, ϕ_2 = 1 and, for measurements at small deformations, A = 1, thus

$$G = \frac{\rho}{M_c} \cdot RT = \frac{N_{ec}}{V_{ec}} \cdot RT = n_{ec} RT \,. \tag{8}$$

Intramolecular Reaction

In network-forming polymerisations, the increasing numbers of reactive groups per molecule, together with the spatial correlations between groups on the same molecule, mean that intramolecular reaction *cannot* generally be neglected. For -A + B- polymerisations, intramolecular reaction can be characterised in terms of the parameter P_{ab} for the smallest loop[2,3,12,13)]

$$P_{ab} = \frac{P(\underline{r} = \underline{0})}{N_{Av}} \,, \tag{9}$$

where $P(\underline{r} = \underline{0})$ is the probability-density of a zero end-to-end vector between reactive groups. P_{ab} thus represents the mutual concentration of A- and B-groups at the ends of the shortest sub-chain that can react intramolecularly. The structure of this sub-chain, consisting of ν skeletal bonds, and of root-mean-square end-to-end distance $\langle r^2 \rangle^{1/2}$, is shown in figure 1. If it assumed that the end-to-end distance distribution can be represented by a Gaussian function, P_{ab} is given by

$$P_{ab} = \frac{1}{N_{Av}} \left\{ \frac{3}{2\pi \langle r^2 \rangle} \right\}^{3/2} . \tag{10}$$

Since the units of P_{ab} are moles per unit volume, it can be described as the mutual *concentration* of a pair of reactive groups on the same molecule that can react intramolecularly, and is said [2,3] to define an *internal* concentration, c_{int}. The concept is shown schematically in figure 2 for an A-group, where the competition between intramolecular and intermolecular reaction

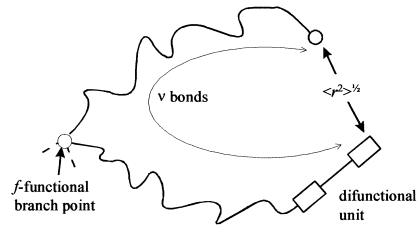

Fig. 1: sub-chain forming a smallest loop structure illustrated with respect to an $RA_2+RB'_f$ polymerisation. The diagram shows the two arms of a star reactant, one arm having reacted with a difunctional monomer; the root-mean-square distance of the chain of ν bonds between the terminal groups is $\langle r^2 \rangle^{1/2}$.

with B-groups is due to the (internal) concentration of B-groups on the same molecule (described by $c_{b,int}$) relative to that of B-groups on other molecules, the so-called external concentration, $c_{b,ext}$. The latter quantity may be approximated by the simple expression

$$c_{b,ext} = c_b = c_{b0}(1 - p_b) \,, \tag{11}$$

where c_b is the instantaneous concentration of reactive groups (at extent of reaction p_b). A

corresponding expression exists for the intermolecular reaction of a B-group, namely

$$c_{a,ext} = c_a = c_{a0}(1 - p_a) \ . \qquad (12)$$

Intramolecular reaction between the pendant A- and B-groups at the ends of the sub-chain shown in Fig. 1 results in the formation of the smallest loop. However, it is apparent that loop sizes, consisting of larger numbers of monomer (reactant) units are possible, resulting in ring structures with integer multiples of v bonds. If all such sub-chains in a polymerisation mixture are assumed to obey Gaussian statistics, the parameter characterising the formation of the i^{th} size of loop can be evaluated using a more general form of equation (10),

$$P_{ab,i} = \left(\frac{3}{2\pi i < r^2 >}\right)^{\frac{3}{2}} \frac{1}{N_{Av}} = P_{ab} . i^{-\frac{3}{2}} . \qquad (13)$$

It is assumed that the presence of i branch points in a sub-chain forming a loop of size i does not disproportionately affect the conformational statistics.

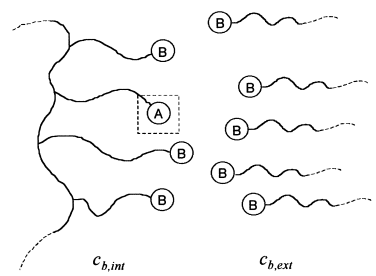

Fig. 2: Illustrating the concepts of internal and external concentrations of B-groups around a chosen A-group, leading, respectively, to intramolecular and intermolecular reaction

A useful measure of the propensity of a system at a given ratio of reactants for intramolecular reaction is λ_{a0}, where

$$\lambda_{a0} = \frac{P_{ab}}{c_{a0}} \ , \qquad (14)$$

with c_{a0} the initial concentration of A-groups. λ_{a0} captures the combined effects of reactant structure and reactive-group concentration. A decrease in chain length or chain stiffness (i.e., a decrease in $<r^2>$) results in an increase in P_{ab} and, hence, in the probability of intramolecular reaction and the formation of loop structures. Similarly, decreasing the concentration of reactive groups enhances the probability of intramolecular reaction.

Experimental Results for Polyurethane (PU) Networks

The results to be discussed come from six series of PU-network materials formed via stoichiometric RA_2+$R'B_f$ polymerisations of hexamethylene diisocyanate (HDI) and star

polyoxypropylene (POP) polyols, at different initial dilutions in nitrobenzene[14,15]. The structure of the polyol ($R'B_f$) was varied in order to examine the effects of branch-point functionality (f) and reactant sub-chain length (ν) on the moduli of the resulting networks. The six reaction systems are listed in Table 1. As described in equation 4, M_c^o is the network-chain molar mass in the perfect network and is defined by the reactant structures. By rearranging the sub-chain illustrated in Fig. 1, it is easy to show that M_c^o is also the molar mass of the sub-chain of ν skeletal bonds[15]. The values of $\langle r^2 \rangle$ listed enable values of P_{ab} to be calculated using equation (10).

Table 1: Functionalities, f, numbers of skeletal bonds, ν, in the sub-chains forming the smallest possible loops and elastic chain molar masses in the perfect networks, M_c^o, for six series of stoichiometric PU-forming, nonlinear polymerisations[15]. The calculated values, using detailed conformational analyses[16], of the mean-square end-to-end distances, $\langle r^2 \rangle$, of the sub-chains of ν bonds embedded in branched structures are also shown.

PU system	f	ν	M_c^o /g mol^{-1}	$\langle r^2 \rangle$ /nm^2
1. HDI + POP triol	3	35	635	3.718
2. HDI + POP triol	3	62	1168	6.877
3. HDI + POP tetrol	4	28	500	2.753
4. HDI + POP tetrol	4	32	586	3.628
5. HDI + POP tetrol	4	43	789	4.605
6. HDI + POP tetrol	4	65	1220	6.581

The plots in Fig. 3 give the values of M_c, relative to M_c^o for the perfect networks (M_c / M_c^o), as functions of the average initial dilution of reactive groups, $2/(ca_0+cb_0)$, for the six series of PU networks formed at complete reaction. The values of M_c were determined from uniaxial compression measurements on dry and swollen networks and analysis of the results using equations (6) and (7). For each of the six experimental systems, an increase in the initial dilution of reactive groups results in greater reductions in moduli, consistent with an increased incidence of intramolecular reaction, and the formation of inelastic loop structures. The positive slopes of the plots indicate that direct relationships exist between intramolecular reaction (which increases with reactant dilution) and the network defects at complete reaction. This in itself shows that the dominant network defects are inelastic loop structures, which can form both pre-gel and post-gel.

The plots in Fig. 3 clearly show that the magnitudes of the experimentally observed reductions in modulus are by no means insignificant. If perfect networks were formed, then

M_c / M_c^o =1. Hence, there is a ten-fold decrease in modulus in the case of the dry (bulk) network formed from the short-chain triol (system 1; M_c^o = 635 g mol^{-1}), at the highest initial

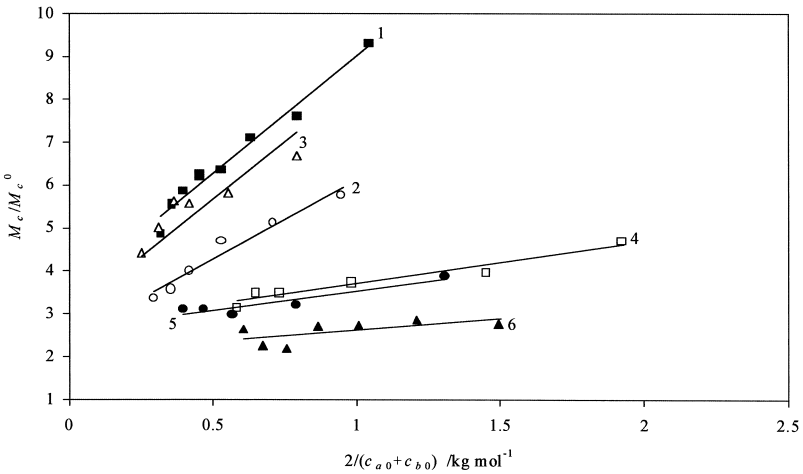

Fig. 3: Experimentally-determined values of M_c / M_c^o at complete reaction as functions of the average initial dilution of reactive groups, $2/(c_{a0}+c_{b0})$, for the six series of PU networks of Table 1.

dilution of reactive groups. For a given branch-point functionality, an increase in sub-chain length (ν) results in a decrease in M_c / M_c^o, due to the decrease in the probability of loop formation (since $\langle r^2 \rangle$ in equation (13) increases). At approximately the same values of ν, the reductions in moduli for tetrafunctional networks are considerably less than those of trifunctional ones. To a first approximation, this can be understood [9], on the basis of the different effects of the smallest loops that can form during $f = 3$ and $f = 4$ polymerisations.

Also, it should be noted that if the *perfect* networks were to exhibit phantom rather than affine behaviour, then $A = (1 - 2/f)$ (equation (7)) and for $f = 3$, $M_c / AM_c^o = 3$, and for $f = 4$, $M_c / AM_c^o = 2$. The observed values of M_c / M_c^o (or M_c / AM_c^o for any value of A) are greater, therefore, than those for perfect networks assuming either affine *or* phantom behaviour.

General Effects of Loops on Elasticity

The effect of the smallest and next smallest loop structures (i = 1,2 in equation (13)) on the loss of network elasticity is illustrated in figure 4 for trifunctional and tetrafunctional networks. In perfect f-functional networks, each junction provides $f/2$ elastic chains. In the case of $f = 3$, each smallest loop structure renders two branch points inelastic (shown as □ in the diagram), which is equivalent to the loss of three elastic chains. For $f = 4$, the effect is reduced; each loop is associated with the loss of a single elastic branch point, or two elastic chains. As a result, trifunctional networks are expected to be the more sensitive to loop defects, and decreases in modulus are expected to be greater than those of tetrafunctional networks with similar values of M_c^o, consistent with the experimental data in Fig. 3.

Unlike the smallest loops, larger loop structures do not disrupt the continuity of the network structure, and therefore network chains in larger loops *are* capable of supporting a load. The examples of the two-membered loop structures for trifunctional and tetrafunctional networks are also shown in figure 3. The question as to *how* larger loop-structures contribute to losses in network elasticity remains unanswered. The conformational entropy of a large loop-structure will be reduced[3,17,18], relative to that of an unperturbed, free linear chain of the same number of skeletal bonds, due to the decrease in the total number of possible

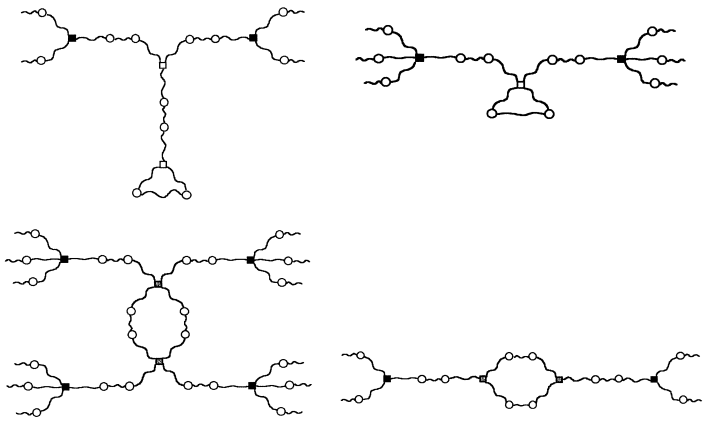

Fig. 4: Smallest (one-membered) and next smallest (two-membered) loop structures (i = 1,2 in equation (13)) in trifunctional and tetrafunctional networks. O represents a reacted pair of groups; ■ denotes a fully-elastic junction point; ▪ denotes a junction point of reduced elasticity; □ denotes an elastically-inactive junction point.

chain conformations resulting from the constraints imposed by the branch points along the chain and at the two chain ends. However, in a *completely reacted* network structure, *every* chain (except those in smallest loops) must form part of a topological circuit, and will therefore be subject to some degree of entropy loss. Since the origin of rubber-like elasticity lies in the conformational entropy of the network chains, any decrease in entropy should manifest itself as a decrease in the elasticity of the real network structure relative to that of the *hypothetical*, perfect one, whose network chains are assumed to be indistinguishable from the corresponding set of unperturbed (free) chains.

Monte-Carlo Polymerisation Algorithm

Theories to predict the modulus of a network material must begin by constructing a realistic model of the network structure, including defects[17,19-21]. Detailed characterisation of the connectivity, or topology, of a network structure by conventional, experimental means is impossible. In order to investigate the effects of network topology on elastomeric properties one must therefore use numerical simulations of the network-forming nonlinear polymerisations. These have the potential to provide this detailed structural information. In such simulations, it is important to account correctly for the formation of loop-structures of various sizes resulting from intramolecular reactions correctly weighted according to their probabilities of formation. To these ends, a Monte-Carlo (M-C) nonlinear polymerisation algorithm, originally devised by Dutton, Stepto and Taylor[17] has been further developed to simulate self-polymerisations (RA_f), and two-monomer polymerisations of the general type RA_2+$R'B_f$. During the course of a simulated polymerisation, populations of monomer units are connected together according to the relative probabilities for intramolecular and intermolecular reactions using λ_{a0} and taking account of possible loop sizes and the decreasing external concentration of reactive groups as a polymerisation proceeds. All the connections are recorded as a function of extent of reaction of A- or B-groups, along with the calculated sol and gel fractions, and average degrees of polymerisation.

The algorithm requires an initial number of A- and B-bearing reactants, $N_a + N_b$ (where $n_{a0} = f_a N_a = n_{b0} = f_b N_b$, for stoichiometric reactions), with functionalities of $f_a = 2$ and $f_b = 3,4$ for the systems to be discussed here. The initial concentrations of reactive groups, c_{a0} and c_{b0}, are also specified. These effectively define a reaction volume for given reactant molar masses. The final parameter characterising the reactants is P_{ab}, so that λ_{a0} (equation (14)) is known.

Loop-Size Distributions and Extents of Intramolecular Reaction

The general description and operation of the algorithm have been described elsewhere[21]. Here, we concentrate on findings relevant to the experimental results in Fig. 3. Accordingly, Fig. 5 shows distributions at complete reaction for an F-S polymerisation and polymerisations with $\lambda_{a0} = 0.01$ and 0.1. The number fraction of loop structures of i repeat units, $n_r(i)$, is plotted against i.

$$n_r(i) = \frac{N_r(i)}{\sum_i N_r(i)} \quad , \tag{15}$$

where $N_r(i)$ denotes the number of loop structures of size i. The F-S simulation was achieved by modifying the algorithm to exclude sol-sol and sol-gel intramolecular reaction and to allow only random intramolecular reaction on the largest species beyond the F-S gel point, i.e., random gel-gel reaction. Smallest loops are negligible under F-S conditions. However, it is clearly seen that smallest loops start to dominate as λ_{a0} increases. Maxima in the distributions reflect the different numbers of opportunities for forming loop structures of various sizes, integrated over all post-gel reaction. Also, the maximum is shifted to slightly smaller loop sizes in the simulations using λ_{a0} compared with those using F-S statistics. This is to be expected since intramolecular reactions are then biased towards the formation of smaller loops.

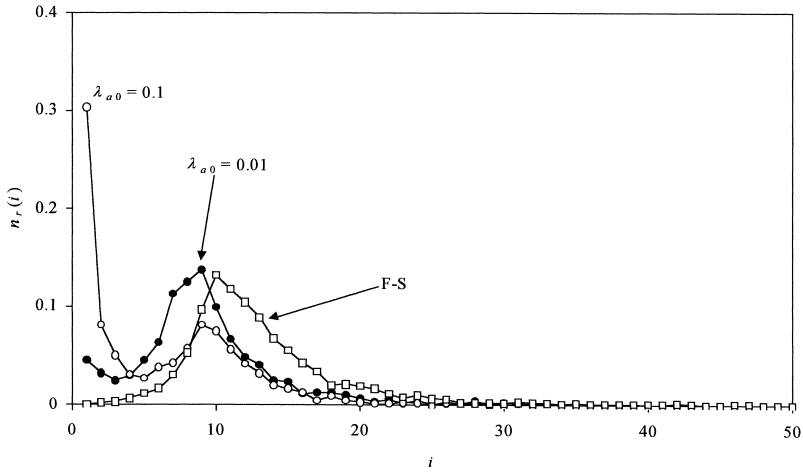

Fig. 5: RA_2+$R'B_4$ simulations at complete reaction. Overall number-fraction loop-size distributions for F-S, $\lambda_{a0} = 0.01$ and $\lambda_{a0} = 0.01$ simulations, each containing 1000 branch units.

The changes in the calculated loop-size distributions in the *gel molecule* at complete reaction with increasing λ_{a0} can be simply characterised by calculating extents of intramolecular reaction on that molecule resulting in smallest loops by the end (*e*) of a polymerisation, $p_{re,1}$, as a function of λ_{a0}. Such a characterisation is useful because the exact effects of smallest loops on network elasticity can be deduced (see Fig. 4). In addition, $p_{re,i>1}$, the extent of reaction resulting in the formation of *larger* loops may also be calculated, so that the total, final extent of intramolecular reaction may be written

$$p_{re,tatal} = p_{re,1} + p_{re,I>1} \quad . \tag{16}$$

Accordingly, series of stoichiometric RA_2+$R'B_3$ and RA_2+$R'B_4$ simulations with 1000 branch units were performed with λ_{a0} in the range 0.01 to 0.40, covering the experimental polymerisations in Fig. 3. For illustration, the results for the series of RA_2+$R'B_3$ simulations are shown in Fig. 6. Notice that $p_{re,tatal}$ = 1/6, always. This is related to the cycle rank of the completed network. For a stoichiometric RA_2+$R'B_f$ polymerisation at complete reaction[22] $p_{re,tatal} = (1/2)(1 - 2/f)$.

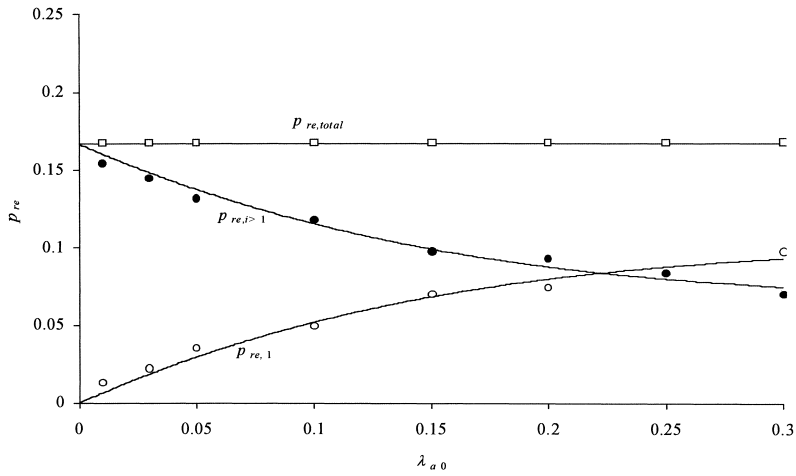

Fig. 6: $p_{re,1}$ and $p_{re,i>1}$ versus λ_{a0} for RA_2+$R'B_3$ simulations with 1000 branch units.

Fig. 6 shows that the incidence of smallest loops ($p_{re,1}$) is negligible when $\lambda_{a0} = 0$. Essentially, in agreement with F-S statistics and the results in Fig. 5, all intramolecular reaction then occurs *after* the gel point, resulting in larger loop structures. However, as λ_{a0} increases, $p_{re,1}$ increases, at the expense of the proportion of larger loop structures ($p_{re,i>1}$). For a given value of λ_{a0}, it is found that tetrafunctional systems give rise to more loop structures than trifunctional systems, simply due to the greater number of opportunities for loop-formation in the former case. However, relative to the *total* number of loop structures, the

proportion of smallest loops appears to be fairly insensitive to the branch-point functionality[21].

Correlation of Model Network Topologies with Measured Network Moduli

The effects of loop structures on experimental reductions in moduli can be taken into account, approximately, by basing the numbers of elastically effective chains on values corresponding to $p_{re,1}$ and $p_{re,i>1}$ from the M-C simulations. If the number of chains rendered elastically ineffective, N_c^I, can be estimated, the reduction in modulus, or increase in M_c, can be calculated using

$$\frac{M_c}{M_c^o} = \frac{N_{ec}^o}{N_{ec}} = \frac{N_{ec}^o}{N_{ec}^o - N_c^I} \quad . \tag{17}$$

From equation 3, $N_{ec}^o = N_J \cdot f / 2$ and the quantity N_c^I may be estimated as follows. For the simulated trifunctional networks of N_J branch units, the numbers of smallest loops are given by $3N_J p_{re,1}$, which equates to a loss of elastic chains equal to $3 \times 3N_J p_{re,1}$. However, the $3 \times 3N_J p_{re,i>1}$ chains in *larger* loops are subject only to a partial loss in elasticity, and may be taken as equivalent to $x \times 3 \times 3N_J p_{re,i>1}$ chains, where x is the fractional loss in elasticity per chain in a larger loop structure. ($x = 1$ corresponds to a *total* loss in elasticity, seen in the case of smallest loops only.) Hence, for $f = 3$

$$N_c^I = \frac{3N_J}{2} \cdot \left(6p_{re,1} + x \cdot 6p_{re,i>1}\right) \tag{18}$$

and substituting for N_c^I and N_{ec}^o in equation (17) yields

$$\frac{M_c}{M_c^o} = \frac{1}{1 - 6p_{re,1} - x \cdot 6p_{re,i>1}} \quad . \tag{19}$$

A similar expression can be derived for tetrafunctional network structures. They lose only 2 elastic chains per smallest loop and

$$\frac{M_c}{M_c^o} = \frac{1}{1 - 4p_{re,1} - x \cdot 4p_{re,i>1}} \quad . \tag{20}$$

Estimates of x, the fractional loss of elasticity for chains in larger loop structures, can be made using the experimentally determined values of M_c / M_c^o for the series of PU networks in Fig. 3, in conjunction with simulated values of $p_{re,1}$ and $p_{re,i>1}$ and equations (19) and (20). However, since $p_{re,1}$ and $p_{re,i>1}$ calculated via the M-C simulations are dependent upon P_{ab},

values of M_c / M_c^o depend on both x *and* P_{ab}. Correlations between M-C calculations and experimental data may therefore be performed in two ways:

i) bivariate least-squares fitting, to evaluate both x and P_{ab}

ii) monovariate least-squares fitting, to evaluate x using P_{ab} values calculated *ab initio*, via chain-conformational analyses[16] and the values of $\langle r^2 \rangle$ in Table 1.

The calculated values of x and P_{ab} for PU systems 1 to 6 are listed in Table 2 and the fittings of the experimental M_c / M_c^o data using the bivariate and monovariate analyses are shown, respectively, in Figs. 7 and 8. The bivariate analysis results in very good fits to the

Table 2: Values of x and P_{ab} based on correlations of experimentally-measured reductions in moduli for PU networks, and extents of intramolecular reaction calculated from M-C simulations. [a]bivariate fitting; [b]monovariate fitting with P_{ab} values calculated *ab initio*, via chain-conformational analyses using $\langle r^2 \rangle$ values from Table 1.

PU system	F	x^a	$P_{ab}{}^a$ /mol l^{-1}	x^b	$P_{ab}{}^b$ /mol l^{-1}
1	3	0.667	0.538	0.816	0.076
2	3	0.599	0.103	0.690	0.030
3	4	0.684	0.547	0.775	0.120
4	4	0.638	0.457	0.730	0.079
5	4	0.582	0.129	0.637	0.055
6	4	0.481	0.088	0.559	0.032

experimental data and values of x in the range 0.67 to 0.60 are required to reproduce the experimental modulus reductions for the trifunctional PU networks (systems 1 and 2), and 0.68 to 0.48 for the tetrafunctional PU networks (systems 3 to 6). In both cases, an increase in the size of the smallest loop structure results in a decrease in x, indicating less elasticity lost. However, the values of P_{ab} estimated from the bivariate fitting are *much higher* than those calculated via $\langle r^2 \rangle$ for the sub-chain structures. Use of the *ab initio* calculated values of P_{ab} in the monovariate analysis results in a worse fitting of the experimental data at the higher values of M_c / M_c^o, but acceptable values of x are still required (x=0.82 - 0.69, for f = 3, and 0.78 - 0.56 for f = 4).

Finally, Fig. 9 illustrates the effects of assuming that x = 0 (*i.e.* no additional loss in elasticity from larger loop structures). The experimental data from system 3 are shown in comparison with the results from the bivariate and monovariate analyses and the monovariate analysis with x = 0. It is obvious that the neglect of the loss of elasticity in larger loop structures results in a *gross underestimation* of the experimentally observed reductions in moduli. The effects of the values used for P_{ab} are secondary compared with the effects of assuming x = 0.

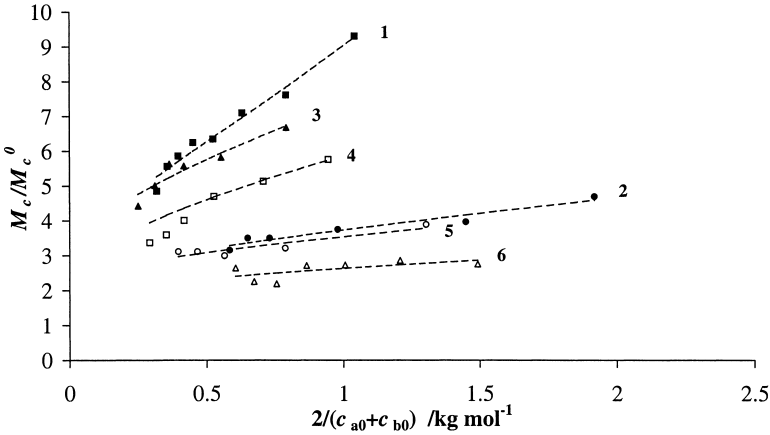

Fig. 7: M_c / M_c^o versus average initial dilution of reactive groups, $2/(c_{a0}+c_{b0})$, for the PU systems of Table 1 and Fig. 3. Experimental values of M_c / M_c^o and calculated values using the bivariate analysis.

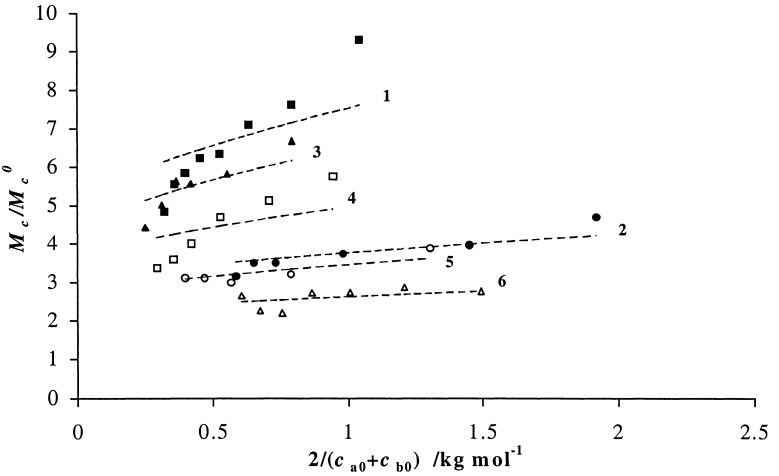

Fig. 8: M_c / M_c^o versus average initial dilution of reactive groups, $2/(c_{a0}+c_{b0})$, for the PU systems of Table 1 and Fig. 3. Experimental values of M_c / M_c^o and calculated values using the monovariate analysis.

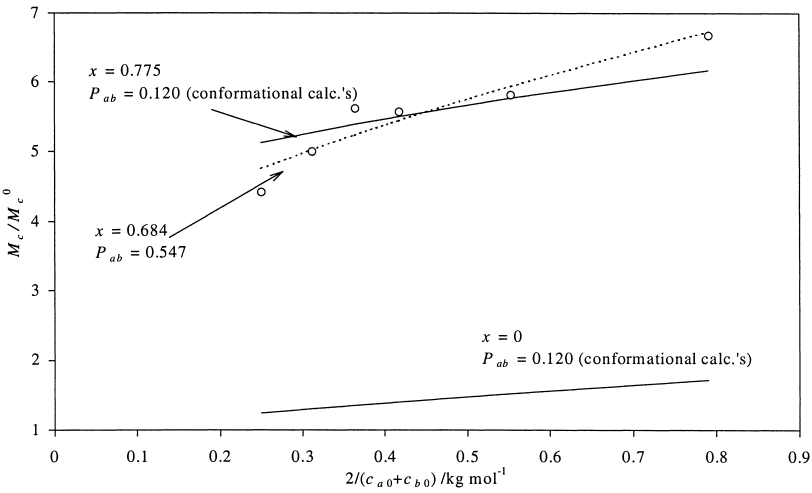

Fig. 9: M_c / M_c^o versus average initial dilution of reactive groups, $2/(c_{a0}+c_{b0})$, for PU system 3 of Table 1 and Fig. 3. Experimental values of M_c / M_c^o and calculated values using the bivariate and monovariate analyses and the monovariate analysis with $x = 0$.

Discussion and Conclusions

Although the incidence of unreacted chain ends in a network material can, in principle, be quantified experimentally, enumerating network defects due to loop structures remains experimentally intractable. An M-C simulation approach, in which the numbers of loop structures formed are weighted according to size and the molecular structures of the reactants, can provide this detailed information, providing a means of generating realistic model network structures, whose topologies are known in full detail.

The correlations described, between experimentally measured network moduli and extents of loop-forming reaction calculated via M-C simulation, show clearly that larger loop structures contribute significantly to the observed loss of elasticity relative to that of a perfect network.Current work is focusing on the direct calculation of the entropies of larger loop structures and more exact calculations of P_{ab} for sub-chains in branched structures. From such calculations, moduli can be predicted more accurately, *directly* from reactant structures and reaction conditions, without the use of semi-empirical value of x and P_{ab}.

Acknowledgement

Support of the EPSRC for grant GR/L/66649 is gratefully acknowledged.

References

1. P.J. Flory, "*Principles of Polymer Chemistry*", Cornell University Press, Ithaca 1953
2. R.F.T. Stepto, in "*Comprehensive Polymer Science*", 1st Suppl., S.L. Aggarwal and S. Russo, eds., Pergamon Press, Oxford, 1992, chap. 10
3. R.F.T. Stepto, in "*Polymer Networks – Principles of Their Formation, Structure and Properties*", R.F.T. Stepto, ed., Blackie Academic & Professional, London, 1998, chap. 2
4. J.E. Mark and B. Erman, in "*Polymer Networks – Principles of Their Formation, Structure and Properties*", R.F.T. Stepto, ed., Blackie Academic & Professional, London, 1998, chap. 7
5. W.W. Graessley, *Adv. Polymer Sci.*, **16** (1974)
6. M. Doi and S.F. Edwards, *J. Chem. Soc., Faraday Trans. 2,* **74**, 1789, 1802, 1818 (1978)
7. G. Heinrich, E. Straube and G. Helmis, *Adv. Polymer Sci.*, **85**, 34 (1988)
8. O. Kramer, in "*Elastomeric Polymer Networks*", J.E. Mark and B. Erman, eds., Prentice Hall, Englewood Cliffs, NJ, 1992, chap. 17
9. R.F.T. Stepto and B.E. Eichinger, in "*Elastomeric Polymer Networks*", J.E. Mark and B. Erman, eds., Prentice Hall, Englewood Cliffs, NJ, 1992, chap. 18
10. M. Gottlieb, C.W. Macosko, G.S. Benjamin, K.O. Meyers and E.W. Merrill, *Macromolecules*, **14**, 1039 (1981)
11. C.W. Macosko and J.C. Saam, *Polymer. Prepr., Div. Polymer Chem., Amer. Chem. Soc.,* **26**, 48 (1985)
12. H. Jacobson and W.H. Stockmayer, *J. Chem. Phys.*, **18**, 1600 (1950)
13. S.B. Ross-Murphy and R.F.T. Stepto, in "*Large Ring Molecules*", J.A. Semlyen, ed., Wiley, Chichester, 1996, chap.16
14. J.L. Stanford and R.F.T. Stepto, in "*Elastomers and Rubber Elasticity, Amer. Chem. Soc. Symp. Series 193*", J.E. Mark and J. Lal, eds., American Chemical Society, Washington D.C., 1982, chap. 20
15. R.F.T. Stepto, in "*Biological and Synthetic Polymer Networks*", O. Kramer, ed., Elsevier Applied Science, Barking, 1988, chap. 10
16. D.J.R. Taylor and R.F.T. Stepto, *to be published*
17. S. Dutton, R.F.T. Stepto and D.J.R. Taylor, *Angew. Makromol. Chem.*, **240**, 39 (1996)
18. W.W. Graessley, *Macromolecules*, **8**(2), 186, 865 (1975)
19. K.-J. Lee and B.E.Eichinger, *Polymer*, **31**, 406, 414 (1990)
20. E.S. Page and L.B. Wilson, "*An Introduction to Computational Combinatorics*", Cambridge University Press,1979, p.74 *et seq*
21. R.F.T. Stepto and D.J.R. Taylor, in "*Cyclic Polymers*", 2nd ed., J.A. Semlyen, ed., Kluwer, 1999, *in press*
22. R.F.T. Stepto, *Polym. Bull. (Berlin)*, **24**, 53 (1990)